Development of Deposition Models for Paint Application on Surfaces Embedded in $\mathbb{R}^3$ for Use in Automated Path Planning

David C. Conner,* Prasad N. Atkar, Alfred A. Rizzi, and Howie Choset

Carnegie Mellon University, Pittsburgh, PA

Abstract

As part of an ongoing collaborative effort with the Ford Motor Company, our research aims to develop practical and efficient trajectory planning tools for automotive painting. This paper documents our efforts to develop analytic deposition models for electrostatic rotating bell (ESRB) atomizers, which have recently become widely used in the automotive painting industry. Conventional deposition models, used in earlier automatic trajectory planning tools, fail to capture the complexity of deposition patterns generated by ESRB atomizers. The models presented here take into account both the surface curvature and the deposition pattern of ESRB atomizers, enabling planning tools to optimize trajectories to meet several measures of quality, such as coating uniformity. In addition to the development of our models, we present experimental results used to evaluate our models, and verify the interaction between the deposition pattern, trajectory, and surface curvature.

1 Introduction

Industrial robots are widely used for automotive paint application. The repeatability of the surface finish, along with the removal of humans from a hazardous environment, are major benefits of robotic application. While applying paint is purely robotic, generating trajectories for the robots is largely a human endeavor based on the experience of skilled technicians. In the automotive industry, uniformity of the final coating thickness is an important measure of quality. Excessive variation is visible to the human eye, and leads to customer rejection [1]. Trajectories that are planned for painting robots must yield paint deposition that is both complete in its coverage, and sufficiently uniform so that the variation in thickness is not noticeable, and does not degrade the coating performance. Since the final trajectories cannot be generated until the body design is finalized, the development of good painting plans represents a bottleneck in the concept-to-customer time line. Any progress in automating this task ultimately decreases the total time required to bring a new concept to the customer.

*corresponding author: dcconner@cmu.edu

In this paper, we outline our first steps toward finding methods to automate the task of planning trajectories given the complicated deposition patterns generated by rotating bell atomizers. Section 2 covers relevant prior work for this research. In Section 3, we develop analytic models of the deposition pattern and variation generated by high speed rotating bell atomizers. We discuss experimental tests and methods used to parameterize and validate the analytic models in Section 4. Finally, in Section 5 we draw conclusions from the results and discuss the future direction of our work.

2 Prior Work

The work that we present in this paper is an outgrowth of our prior work in the area of coverage planning [2]. The earlier work developed plans for guaranteeing complete coverage of an unknown area, and was later lifted to surfaces embedded in $\mathbb{R}^3$ [3]. While this prior work guaranteed complete coverage, it did not necessarily yield uniform coverage. Our work now focuses on the task of planning trajectories in a way that guarantees complete coverage, while at the same time minimizing coating variation.

There have been several attempts to develop trajectory planners for painting robots, but none have been widely adopted for industrial use. An early attempt, the Automatic Trajectory Planning System (ATPS), was limited by its use of a simplified deposition model [4]. Other researchers have proposed systems for generating trajectory plans based on CAD data, but they all require user decisions regarding the effect of surface shape on trajectory parameters [5, 6]. Several researchers have proposed high level frameworks for solving the trajectory planning problem, but do not include realistic models of the deposition pattern and its interaction with surface curvature [7, 8].

Research on more sophisticated deposition patterns has assumed the use of aerosol atomizers, which generate deposition patterns that are not compatible with the patterns generated by ESRB atomizers. Arikan and Balkan developed a paint deposition simulation where the paint deposition model used a beta distribution [9]. Their work considered the effect of the paint deposition pattern on

the optimal distance between consecutive passes of the paint atomizer, along with a preliminary attempt at considering surface effects on the deposition. Hertling *et al.* proposed more realistic deposition models for use in their trajectory planning system, but specifically limited their work to aerosol sprays citing the inherent complexity of electrostatic deposition patterns [10].

Automotive coating processes are moving increasingly towards the use of ESRB atomizers in order to increase transfer efficiencies [11, 12, 13]. Researchers developing models of the deposition of paint by ESRB atomizers have generally focused on electrostatic effects, and the interaction between the electric fields and the charged paint droplets. Early work in modeling the electrical effects of these ESRB systems was performed by Elmoursi [12], and later expanded by Ellwood and Braslaw to include coupling between the droplet flow and the electrical field [11].

3 Deposition Modeling

The deposition model developed in this paper has two primary purposes: *i*) to capture the structure of the deposition pattern for use by planning tools, and *ii*) to support simulations that accurately predict the results of specific atomizer trajectories. These two purposes lead to contradictory criteria for evaluating the model. First, the model must be accurate enough to capture the structure of the deposition and accurately predict the deposition on a variety of surface shapes. However, the model must be tractable from the perspective of the simulation and planning tools.

In an ESRB atomizer, paint fluid is forced onto the inner surface of a high speed rotating bell [11, 12]. The bell is maintained at a high voltage of 40-90 kV relative to the grounded surface being painted. Most modern systems use negative polarity at the atomizer [1]. The paint flow breaks up at the edge of the bell, forming a cloud of droplets, as it is expelled radially due to centrifugal force imparted to the paint by the rotating bell. Each paint droplet is electrically charged due to the charge on the bell. High velocity shaping air and a charged pattern control ring are used to force the charged droplets towards the grounded surface being painted. Figure 1 shows a schematic of a typical atomizer configuration.

As the atomizer passes over the surface, the majority of the paint emitted by the atomizer is deposited on the surface, although some paint is inevitably entrained in the shaping air and lost. For the ESRB atomizers studied in this paper, the overall shape of the deposition pattern is roughly circular when the bell is oriented normal to a flat panel and the atomizer is stationary; we refer to this as the *2D deposition pattern*. As the bell moves relative to the surface, the 2D deposition pattern moves over the surface and paint is accumulated on the surface. The resulting paint thickness profile, which we refer to as the *1D col-*
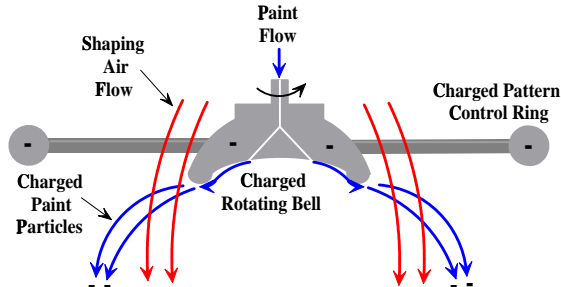

Figure 1: *Electrostatic rotating bell atomizer with paint particle trajectory and shaping air flow lines shown.*

lapse, is equivalent to that obtained by integrating the deposition model along the direction of travel [14]. Figure 2 shows the relationship between the 2D deposition pattern and the resulting 1D collapse generated by the motion of the atomizer.

3.1 Deposition Flux Model

We seek a deposition model that assigns the rate of paint deposition or *deposition flux* at a given point on an arbitrary surface, given a specific location and orientation of the atomizer [10]. The model we developed, denoted $D(\mathbf{s}, \mathbf{p})$, is of the form $D : \{\mathbb{R}^3 \times \mathbf{S}^2\} \times \mathrm{SE}(3) \to \mathbb{R}$, where $\mathbf{s}$ is a point and unit surface normal on the surface being painted and $\mathbf{p} \in \mathrm{SE}(3)$ is the location and orientation of the bell atomizer. We refer to $D(\mathbf{s}, \mathbf{p})$ as the *2D deposition model*, or simply the *deposition model*.

Parameterizing the deposition model for arbitrary surfaces is difficult at best. Since experimental data for planar surfaces is readily available, we developed an analytic model for the deposition flux on a planar surface. We parameterize this model based on experimental data, and then use the parameterized planar model to predict paint deposition flux on the surface being painted. We refer to the analytic model for the planar surface as the *planar deposition model*. The planar surface, oriented normal to the atomizer and located a fixed distance from the atom-
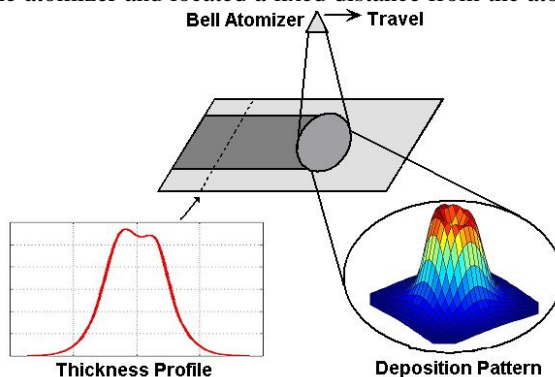

Figure 2: *Painting a flat panel, with detail of the 1D collapse (l) and the and the 2D Deposition pattern (r).*

izer emission point, is referred to as the *deposition model plane* and is shown in Figure 3.

We denote the planar deposition model as $d(\mathbf{q}) = d(x,y)$, where $d : \mathbb{R}^2 \to \mathbb{R}$, and $\mathbf{q} = (x,y)$ is the point on the deposition model plane. The point $\mathbf{q}$ is dependent on the deposition model plane, the location and orientation of the atomizer, and the surface point. The planar deposition model that we developed uses two Gaussians: one offset 1D Gaussian revolved around the origin and one 2D centered Gaussian. The resulting planar deposition model, similar to the asymmetric volcano shown in Figure 2, is given by

$$d(x,y) = K_1 \left((1 - K_2) \ f(x,y) \ g_1(x,y) + K_2 \ g_2(x,y) \right) , \qquad (1)$$

where K_2 weights the revolved Gaussian against the centered Gaussian and $0 < K_2 < 1$.

To account for asymmetry in the deposition pattern, the revolved offset Gaussian, $g_1 : \mathbb{R}^2 \to \mathbb{R}$, is scaled by the function $f : \mathbb{R}^2 \to \mathbb{R}$. We define f to be

$$f(x,y) = (1 + K_3 \ \sin(\operatorname{atan2}(y,x) - \phi)) ,$$

where K_3 weights the asymmetry scaling function for the revolved Gaussian and $0 < K_3 < 1$. The phase angle, ϕ, allows the asymmetry to be localized relative to the atomizer reference frame. K_1 scales the resulting deposition pattern to give the paint deposition flux in units of thickness per second.

The revolved offset Gaussian, g_1, is defined to be

$$g_1(x,y) = \frac{1}{\gamma} \left(\exp\left(-\frac{\left(\sqrt{x^2+y^2}-r\right)^2}{2\sigma_1^2} \right) + \exp\left(-\frac{\left(\sqrt{x^2+y^2}+r\right)^2}{2\sigma_1^2} \right) \right) ,$$

where r is the offset radius, σ_1 is the standard deviation of the Gaussian, and γ normalizes the revolved Gaussian deposition pattern such that the integral of g_1 over x and y equals one. The scaling factor γ is given by

$$\gamma = 2\pi \left(2\sigma_1^2 \exp\left(-\frac{r^2}{2\sigma_1^2} \right) + r\sigma_1\sqrt{2\pi} \ \operatorname{erf}\left(\frac{r}{\sqrt{2} \ \sigma_1} \right) \right) .$$

The centered Gaussian, $g_2 : \mathbb{R}^2 \to \mathbb{R}$, which is also normalized, is defined to be

$$g_2(x,y) = \frac{1}{2\pi\sigma_2^2} \ \exp\left(-\frac{x^2+y^2}{2\sigma_2^2} \right) ,$$

where σ_2 is the standard deviation of the centered Gaussian.

We extend the planar deposition model to arbitrary surfaces, located at varying offset distances and orientations, by projecting the deposition flux from the deposition model plane onto the surface in a way that preserves
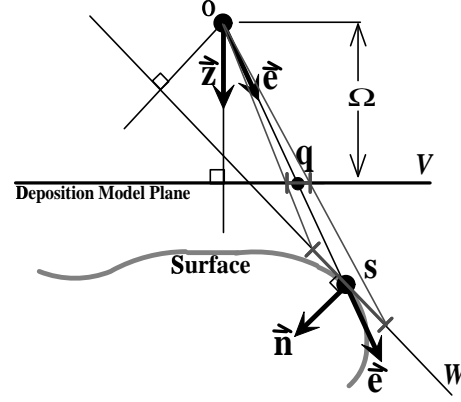

Figure 3: *Projection of deposition model onto arbitrary surface. Although the vectors are in reality three dimensional, this simple figure conveys the basic results.*

the total paint volume. The projection model, shown in Figure 3, is developed by assuming a point source, called the emission point, constrained to lie along the bell to surface vector, $\vec{z}$. Note, this emission point, denoted $\mathbf{o}$ (for origin) in Figure 3, is a theoretical emission point, not necessarily coincident with the bell atomizer center point. The emission point is located relative to the atomizer path location. The deposition model plane is defined to be a distance Ω from the emission point along the bell to surface unit vector, $\vec{z}$. A vector from the emission point to a point $\mathbf{s}$ on the surface passes through the deposition model plane at point $\mathbf{q}$. It is assumed that the planar deposition $d(\mathbf{q}) = d(x,y)$, as defined in (1), is known for a given point (x, y, Ω) on the deposition model plane defined in Figure 3. Furthermore, we assume that the x-y frame of the planar deposition model is aligned with the x-y plane of the atomizer reference frame.

A differential element on the deposition model plane gives a paint solids volume of $V = d(\mathbf{q}) \, dx \, dy$. As this differential element is projected onto the surface about point $\mathbf{s}$, the total volume must remain unchanged in order to preserve mass (assuming constant solids density). We will derive the required relationship using the differential geometry concept of area magnification [15].

Given a path location $\mathbf{p}$ which determines $\mathbf{o}$ and $\vec{z}$, a surface point $\mathbf{s}$, and surface normal $\vec{n}$, we can determine $\vec{e}$, $\mathbf{q}$, and $L = \|\overline{\mathbf{os}}\|$. Using these, we define the deposition flux, $D(\mathbf{s}, \mathbf{p})$, at point $\mathbf{s}$ on the surface being painted to be equivalent to the deposition flux at point $\mathbf{s}$ on the plane tangent to the surface at $\mathbf{s}$. It follows that $D(\mathbf{s}, \mathbf{p})$ is given by

$$D(\mathbf{s}, \mathbf{p}) = \frac{\Omega^2 \langle \vec{e}, \vec{n} \rangle}{L^2 \langle \vec{e}, \vec{z} \rangle^3} d(\mathbf{q}) , \qquad (2)$$

where $d(\mathbf{q})$ is the deposition flux at point $\mathbf{q}$ on the deposition model plane.[1] The reader is referred to [14] for a

---

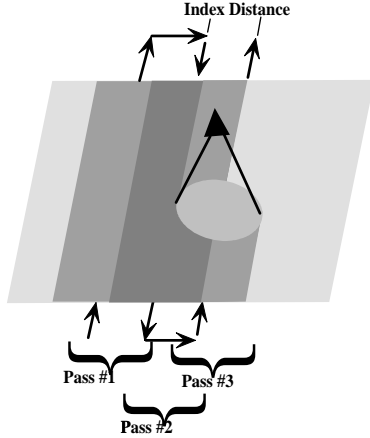[1] The $< \cdot, \cdot >$ notation refers to the standard inner product.

Figure 4: *Painting a flat panel with 3 passes.*

detailed derivation of this result.

3.2 Thickness Variation Model

In order to control the amount of variation in the coating thickness, the trajectory planner must know the relationship between the deposition pattern of the atomizer and the deposition on the surface being painted. For painting specialists, this knowledge is intuitive and based on years of experience. To automate the process of generating these trajectories, we need a computable understanding of the relationship between deposition patterns and thickness variation.

Typically, the deposition pattern is narrow compared to the width of the surface being painted, and requires multiple passes to completely cover the surface as shown in Figure 4. In order to develop plans in a systematic manner, it is desired to know the thickness variation for various indexes. Initially, we will restrict ourselves to a flat panel. We assume that the robot is moving in a straight line, and that the path is sufficiently long so that effects due to turning are negligible.[2]

Unfortunately, the complexity of the analytic model renders the calculation of an analytic integral intractable. Instead, we directly define the 1D collapse model using three separate Gaussians. Two Gaussians are offset from the centerline to allow asymmetries in the deposition pattern to be modeled, while the third Gaussian is centered. The complete 1D collapse model is given by

$$
\begin{aligned}
c(x) \;=\; \frac{1}{3\sqrt{2\pi}} \Big(\; & \frac{1}{\sigma_1} K_1 \, \exp\left(-\frac{(x-r_1)^2}{2\sigma_1^2}\right) + \\
& \frac{1}{\sigma_2} K_2 \, \exp\left(-\frac{(x+r_2)^2}{2\sigma_2^2}\right) + \quad (3) \\
& \frac{1}{\sigma_3} K_3 \, \exp\left(-\frac{x^2}{2\sigma_3^2}\right) \Big),
\end{aligned}
$$

where r_i represents the offset radii, σ_i represents the stan-

---

[2]The question, 'What is sufficiently long?', is answered relative to the diameter of the deposition pattern.
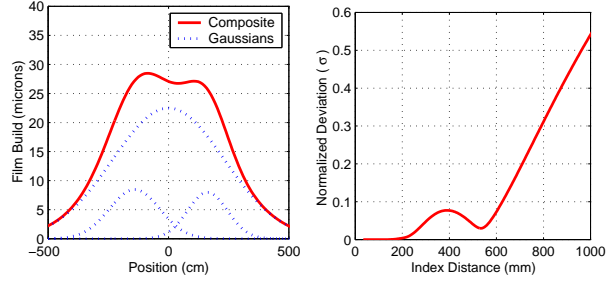

Figure 5: *(l) Asymmetric 1D collapse model with component Gaussians shown. (r) Deviation vs. index distance for typical 1D collapse model on a flat surface.*

dard deviations, and K_i represents the gains specifying the paint thickness for each Gaussian. Figure 5 shows the component Gaussians and the composite film build for a particular parameterization of (3).

To determine the variation as a function of the index distance between consecutive paint passes, we will assume an infinite plane painted by an infinite number of passes with the atomizer at a consistent orientation relative to the plane and moving at a constant speed. For a given location x on the interior of the plane, along a line perpendicular to the direction of travel, the total thickness is given by

$$
T(x) = \sum_{i=-\infty}^{\infty} c(x + i\,\Delta x), \qquad (4)
$$

where Δx is the index distance, and $c(\cdot)$ is the 1D collapse model for the given speed and orientation relative to the direction of travel.

Looking at the thickness measurements as we vary x, the thickness profile is periodic with a period equal to the index distance. The normalized variation over one index, with respect to the average thickness $\overline{T}$, is given by

$$
\sigma_N^2 = \frac{1}{\Delta x} \int_{-\frac{\Delta x}{2}}^{\frac{\Delta x}{2}} \left(\frac{T(x)}{\overline{T}} - 1\right)^2 \, dx. \qquad (5)
$$

The integral is tractable and leads to terms involving the error function, $\mathrm{erf}(\cdot)$. We are able to evaluate the structural effects of a given model on variation as we vary the index distances using (5). A typical normalized deviation (σ_N) versus index distance curve is shown in Figure 5. The full development of these variation calculations for planar surfaces, along with the extension to cylindrical surfaces, can be found in [14].

4 Results

To validate the developed models, a series of tests were conducted in an industrial paint shop, using an ABB S3 robot with an ABB 50 mm Micro-Micro Bell atomizer attached. The applied paint was a solvent based automotive paint. The operating conditions of the application
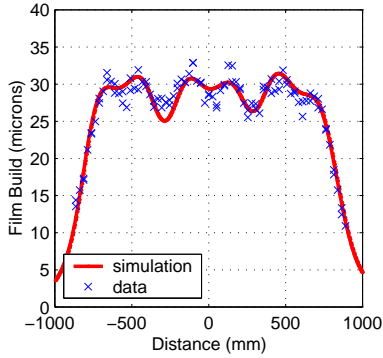
Figure 6: *Deposition simulation using triangulated surface elements at 577 mm index. The simulation captures the inherent structure of the actual deposition pattern. (standard deviation = 1.31 microns)*

process were 80-90 kV electrostatic voltage (negative polarity), 150 cc/min fluid flow, 250 l/min shaping air flow, and a bell speed of 30 kRPM.

4.1 Deposition Model Parameterization

In order to parameterize the 1D collapse and 2D deposition models, experimental data was gathered from flat panels painted by three passes. We chose to parameterize our models using a 577 mm index distance for this three pass test. Given the 577 mm index data, we used numeric optimization to determine the parameters of the 1D collapse. The maximum of the two offset radii and maximum standard deviation from the 1D collapse model were then used to initialize the 2D deposition model parameters.

Given a parameterization of the 2D deposition model, we calculated the 1D collapse thickness values for the parameterized 2D model using numeric integration. The 1D collapse values were then compared to the experimental data. We again used numeric optimization to find the 2D deposition model parameter set that minimized the sum squared error between the experimental data and the numerically integrated 1D collapse. The parameterized models were shown previously in Figures 2 and 5. Figure 6 shows the resulting profile (1D collapse) obtained from a simulation using the 2D deposition model against the data to which it was fit. The simulation results were obtained through numeric evaluation of our deposition models, and give a good match to the experimental data.

4.2 Planar Deposition Results

The parameterized model, fit from the 577 mm index three pass test, was used to predict deposition for other indices. Tests for both 525 and 625 mm indices were conducted with the results shown in Figure 7. The model gives a good prediction of both average film build and the structure of the variation for these flat panel tests. Most importantly, the model captured both the asymme-
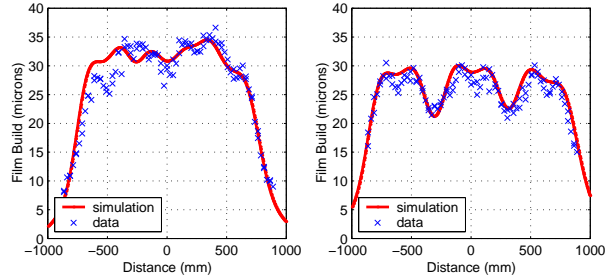

Figure 7: *Deposition simulations at (l) 525 mm index and (r) 625 mm index both using model obtained by 577 mm index test. In both cases, the simulation captures the variation due to the structure of the deposition pattern. (standard deviation = 2.41 and 1.68 microns respectively)*

tries and the structural variation dependence on index distance.

4.3 Surface Deposition Results

The next step in the process was to verify the projection of the planar deposition model from flat panels at constant offset to arbitrary surfaces. To test the deposition on curved surfaces, we used truck doors. Figure 8 shows a CAD model of the truck door used, with a representative path shown. The door has a line of convex curvature near the middle, with a pronounced concave curvature on the bottom third of the door. A series of tests were conducted using both horizontal and vertical passes over the door. For the horizontal passes, film build measurements were taken in four vertical columns of data spread across the door, numbered top to bottom. For the vertical passes, the measurements were taken from six rows spread vertically over the door spaning left to right across the door. Figure 8 shows typical results for the first horizontal test, along with the simulated deposition for each individual pass.

Near the top of the door, in the relatively flat portion, the simulation gives somewhat reasonable results. However, the simulation fails to accurately predict paint thick-
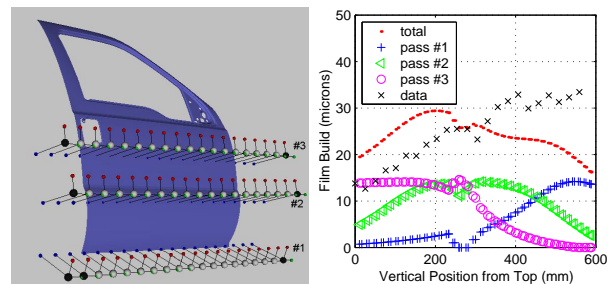

Figure 8: *(l) Door with horizontal paint path shown. The robot paints left to right starting at the left of pass #1, then travels right to left along pass #2, finishing by going left to right along pass #3. (r) Horizontal painting motion on door showing deposition of each pass.*

ness in the highly curved section near the bottom of the door. Clearly the pass along the lower portion of the door deposits more paint than the simulation predicts. It is theorized that when the surface curves away from the bell, electrostatic effects dominate invalidating the geometric projection model developed in Section 3.1. Similar tests, with comparable results, were conducted for vertical painting motions. The reader is referred to [14] for a complete discussion of the results.

5 Conclusions

The results of our experimental studies confirm both the structure of our planar deposition model and the dependence of the thickness variation on that structure. The models we developed accurately predict deposition on planar surfaces, where the atomizer is oriented normal to the surface. Additionally, our analytic 1D collapse model effectively predicts the dependence of the thickness variation on the index distance between passes. Furthermore, the experimental results from deposition on the curved surface of the door confirms the interaction of the surface curvature with the planar deposition pattern, and the resulting change in the deposition pattern on the surface.

Despite the shortcomings of our 2D deposition model, which result from the simplified geometric projection developed in Section 3.1, the model sufficiently captures the structural aspects of the deposition pattern while maintaining an analytic form. By using an analytic model, we are able to develop our understanding of the interaction between the surface, the deposition pattern, and the atomizer path. This enables our exploration of path planning techniques to influence overall quality measures such as thickness variation, cycle time, and efficiency. Since the main focus of our research is on path planning, we will continue to use these analytic models during the development phase of our planning tools. Because our planning tools rely only on the structure of the deposition on the surface, and not on the underlying details of the model used to determine that structure, the need for more expensive models or experimental data is delayed until the implementation stage.

References

[1] Jacob Braslaw. personal communication, 2001.

[2] Ercan U. Acar, Howie Choset, Alfred A. Rizzi, Prasad N. Atkar, and Douglas Hull. Exact Cellular Decompositions in Terms of Critical Points of Morse Functions for Sensor-based Coverage Tasks. *The International Journal of Robotics Research*, accepted for publication 2001.

[3] Prasad N. Atkar, Howie Choset, Alfred A. Rizzi, and Ercan U. Acar. Exact Cellular Decomposition of Closed Orientable Surfaces Embedded in $\mathbb{R}^3$. In *IEEE Int'l. Conf. on Robotics and Automation*, Seoul, Korea, May 2001.

[4] Suk-Hwan Suh, In-Kee Woo, and Sung-Kee Noh. Development of An Automated Trajectory Planning System (ATPS) for Spray Painting Robots. In *IEEE Int'l. Conf. on Robotics and Automation*, Sacramento, California, USA, April 1991.

[5] Naoki Asakawa and Yoshimi Takeuchi. Teachless Spray-Painting of Sculptured Surface by an Industrial Robot. In *IEEE Int'l. Conf. on Robotics and Automation*, Albuquerque, New Mexico, USA, April 1997.

[6] Weihua Sheng, Ning Xi, Mumin Song, Yifan Chen, and Perry MacNeille. Automated CAD-Guided Robot Path Planning for Spray Painting of Compound Surfaces. In *IEEE/RSJ Int'l. Conf. on Intelligent Robots and Systems*, 2000.

[7] Ramanujam Ramabhadran and John K. Antonio. Fast Solution Techniques for a Class of Optimal Trajectory Planning Problems with Applications to Automated Spray Coating. *IEEE Transactions on Robotics and Automation*, Vol. 13(4), August 1997.

[8] Eckhard Freund, Dirk Rokossa, and Jürgen Roßmann. Process-Oriented Approach to an Efficient Off-line Programming of Industrial Robots. In *IECON '98: Proceedings of the 24th Annual Conference of the IEEE Industrial Electronics Society*, volume 1, 1998.

[9] M. A. Sahir and Tuna Balkan. Process Modeling, Simulation, and Paint Thickness Measurement for Robotic Spray Painting. *Journal of Robotic Systems*, Vol. 17(9), 2000.

[10] Peter Hertling, Lars Høg, Rune Larsen, John W. Perram, and Henrik Gordon Petersen. Task Curve Planning for Painting Robots — Part I: Process Modeling and Calibration. *IEEE Transactions on Robotics and Automation*, Vol. 12(2), April 1996.

[11] Kevin R. J. Ellwood and J. Braslaw. A Finite-Element Model for an Electrostatic Bell Sprayer. *Journal of Electrostatics*, Vol. 45(1), 1998.

[12] Alaa A. Elmoursi. Electrical Characterization of Bell-Type Electrostatic Painting Systems. *IEEE Transactions on Industry Applications*, Vol. 28(5), October 1992.

[13] Hua Huang and Ming-Chai Lai. Simulation of Spray Transport from Rotary Cup Atomizer using KIVA-3V. In *ICLASS 2000*, Pasadena, California, USA, July 2000.

[14] David C. Conner, Prasad N. Atkar, Alfred A. Rizzi, and Howie Choset. Deposition Modeling for Paint Application on Surfaces Embedded in $\mathbb{R}^3$ for use in Automated Trajectory Planning. Technical Report CMU-RI-TR-02-08, Carnegie Mellon, Robotics Institute, Pittsburgh, Pennsylvania, USA, June 2002.

[15] J.A. Thorpe. *Elementary Topics in Differential Geometry*. Springer-Verlag., New York, NY, 1979.